SYSTEM LIMIT: THE ULTIMATE CAPACITY OF FRACTIONATORS

Walter J. Stupin and Henry Z. Kister

Fluor Daniel, Aliso Viejo, California

ABSTRACT

The system limit is reached when the superficial vapor velocity in the tower exceeds the settling velocity of large liquid droplets. At higher vapor velocities, ascending vapor lifts and carries over much of the tray liquid, causing the tower to flood. This flood cannot be debottlenecked by improving the internals or by increasing tray spacing. The system limit represents the ultimate capacity limit of the vast majority of the existing trays and of all the existing packings. In some applications, where very open packings or trays are used, such as refinery vacuum towers, the system limit is the actual capacity limit. Until recently no published methods were available to predict it. The factors that affect it are poorly understood.

In the late 1950's and early 1960's, FRI systematically studied this limit in a 1.22 meter diameter column and developed several different correlations. Publication of this first commercial scale "system limit" data by FRI last year permitted us to explore this system limit, shedding much-needed new light on this phenomenon.

The Stupin correlation, based on a dispersed liquid phase falling through an ascending vapor phase, was shown to give excellent prediction of experimental data on the ultimate capacity in the liquid rate range of 40–140 $m^3/h\text{-}m^2$ tower cross section area. However, the correlation tends to predict high at lower liquid rates. The current paper extends Stupin's previous model into the low liquid rate region.

The Ultimate Capacity is a useful concept and represents the limiting vapor velocity independent of tray parameters. This paper extends the earlier correlation of Stupin to lower liquid rates. This correlation provides a useful means to check the limiting capacity that could be expected for a given column diameter and set targets for the capacities of new devices. The challenge is to develop devices that exceed this capacity limit.

BACKGROUND

The system limit is reached when the superficial vapor velocity in the tower exceeds the settling velocity of large liquid droplets. At higher vapor velocities, ascending vapor lifts and carries over much of the tray liquid, causing the tower to flood. This flood cannot be debottlenecked by improving the internals or by increasing tray spacing. The system limit represents the ultimate capacity limit of the vast majority of the existing trays and of all the existing packings. In some applications, where very open packings or trays are used, such as refinery vacuum towers, the system limit is the actual capacity limit.

Improvements in tray hardware over the last couple of decades have brought the capacity of many modern trays close to the system limit. More and more trays approach the system limit at the common tray spacing 600-900 mm. A few new tray devices are even being introduced in which cyclone settling replaces gravity settling, and those can lead to capacities beyond the system limit. Challenging and beating the system limit is the direction in which the mass transfer hardware is headed.

It is amazing that such an important limit received very little attention in the literature. It rates hardly a mention in most distillation texts. Until Recently no published methods were available to predict it. The factors that affect it are poorly understood.

In the late 1950's and early 1960's, FRI systematically studied this limit in a 1.22 meter diameter column. High open area dualflow trays were studied at various tray spacings. As the tray spacing was increased the capacity reached a limit. Publication of this first commercial scale system limit data by FRI, in 2001 (1), permitted us to explore this system limit, shedding much-needed new light on this phenomenon. This paper merges FRI's data with our experience to develop an understanding of the mechanisms defining the system limit, the factors that affect it, and its prediction for commercial scale fractionators. This understanding and predictions are central to improving, designing, debottlenecking and troubleshooting today's and tomorrow's high-capacity trays and packings. A number of other capacity data in the literature were reviewed but the FRI ultimate capacity data are the only known tests that establish such an Ultimate Capacity in commercial scale equipment.

PREVIOUS WORK

The original work of Souders and Brown related the capacity of fractionators due to entrainment flooding to the settling velocity of drops (12). The specific drop size was not calculated but the Souders and Brown constant was determined empirically for an "average" suspended drop. Stichlmair (13) developed a correlation based on the breakup of the liquid on trays into drops by the vapor jet flowing through the holes on the tray. These drops were then entrained by the vapor to the tray above.
The above works and many others in the literature focus on correlations of the capacity of specific devices.

The concept of an Ultimate Capacity or System Limit was developed by Tek (2) while consulting to F.R.I.(Fractionation Research Inc.). The Ultimate Capacity or System Limit is the maximum capacity of counter flow devices (trays or packings) and is based on balancing the force of gravity against the drag forces generated by the vapor. The Tek concept was that the turbulent vapor flow in the inter tray space would break up the liquid into drops and then the vapor would suspend the drops at flood due to the drag.

K. H. Hachmuth of Phillips Petroleum Company proposed to Stupin of FRI (3) the correlation parameter of

$$(\sigma\Delta\rho/\rho_v^2)^{1/4}$$

Stupin (4), while working at FRI, then developed an improved model and correlation, which was based on this parameter, by relating the Ultimate Capacity to the terminal velocity of large drops. The correlation used the equation derived by Levich for the limiting settling velocity for large drops (5). This correlation was shown (1, 2) to give excellent prediction to experimental data on the Ultimate Capacity in the liquid rate range of 40 to 140 m^3/hm^2 tower cross section area.

Stupin (4), and later Fitz and Kunesh (1), noted that the correlation tends to predict high at lower liquid rates, but until recently there were not enough experimental data to extend it into the low liquid rate region. The paper by Fitz and Kunesh made valuable FRI data available in this region. Based on these data, our paper extends Stupin's previous model into the low liquid rate region.

LIMITING OR TERMINAL VELOCITY IN A COLUMN

Much of the fundamental development work reported in this section is Stupin's previous work, detailed in reference (4).

Since the ultimate capacity is independent of tray design and spacing, it is associated with a phenomenon occurring in the inter tray space. This inter tray space is populated with drops of a wide distribution of sizes. In the inter tray space between trays without downcomers, there is a net flow at liquid downward through the turbulently chaotic spray. At the ultimate capacity this net motion relative to the vapor can be represented by the terminal velocity of some effective average drop.

Representing the velocity of the liquid as a terminal velocity of single drop the superficial velocities in a distillation column are related to the superficial velocities by :

$$V_S = (1 - F)\, V_a \qquad (1)$$

$$L_S = F\, L_a \qquad (2)$$

where

V_a = actual vapor velocity

L_a = actual liquid velocity

F = fraction of the flow area occupied by the liquid

By referring to the following diagram, the terminal velocity is:

$$\Delta u = (V_a + L_a)_{ult} \tag{3}$$

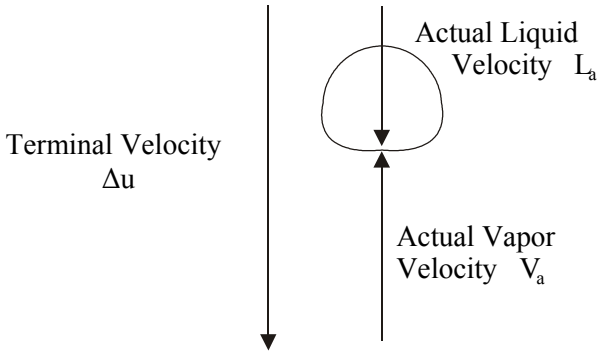

Combining these equations:

$$V_{S,ult} = (1-F)\,\Delta u - \left(\frac{1-F}{F}\right) L_S \tag{4}$$

This equation relates the superficial vapor and liquid velocities to holdup and the terminal velocity.

Writing equation 4 in terms of the capacity factor, gives:

$$C_{S,ult} = V_{S,ult}\left(\frac{\rho_V}{\Delta\rho}\right)^{1/2} = (1-F)\,\Delta u\left(\frac{\rho_V}{\Delta\rho}\right)^{1/2} - \frac{1-F}{F}\left(\frac{\rho_V}{\Delta\rho}\right)^{1/2} L_S \tag{5}$$

Analyzing experimental data on the capacity of high open area dualflow trays at high tray spacing, Stupin (4) showed that over the range of liquid rates considered

$\left(\frac{1-F}{F}\right)\left(\frac{\rho_V}{\Delta\rho}\right)^{1/2}$ is a constant equal to:

$$\left(\frac{1-F}{F}\right)\left(\frac{\rho_V}{\Delta\rho}\right)^{1/2} = 1.40 \tag{6}$$

This equation implies that the liquid holdup at flood is constant in a system in which the liquid is flowing downward as a dispersed phase distributed across the upward flowing vapor. Further this holdup is a function of only the vapor density and the difference between the liquid and the vapor densities and not the rates.

The ultimate capacity correlation is based on combining equations 5 and 6 with the terminal velocity equation. The Levich (5) equation for the settling for large drops is (The derivation of this equation is included in the appendix of this report.)

$$\Delta u=(4g/C_D)^{1/4}(\sigma\Delta\rho/\rho_v^2)^{1/4} \quad (7)$$

Using equations 5, 6 and 7, a drag coefficient was calculated for each ultimate capacity data point. These calculations showed that C_D from varies from about 0.7 to 1.2 for the ultimate capacity data measured by FRI. C_D is probably a complex function of the physical properties. For engineering purposes, an adequate correlation of ultimate capacity is obtained using an average value of C_D equal to 1.0. This approximation does not introduce serious errors since the drag coefficient is taken to the ¼ power. (See the appendix for numerical values of $(4g/C_D)^{1/4}$).

Combining equations 5 and 7,

$$V_{s,ult} = (1-F)(4g/C_D)^{1/4}(\sigma\Delta\rho/\rho_v^2)^{1/4}-((1-F)/F)L_S \quad (8)$$

The holdup terms in equation 8 can be evaluated from equation 6 as:

$$(1-F)/F = 1.4(\Delta\rho/\rho_v)^{1/2} \quad (9)$$

and

$$F = 1/(1+1.4(\Delta\rho/\rho_v)^{1/2}) \quad (10)$$

Combining equations 8, 9 and 10, simplifying and converting to the Souders and Brown (12) capacity factor gives:

$$C_{S,ult} =V_{S,ult} (\rho_v/\Delta\rho)^{1/2} = (1.4/(1+1.4(\Delta\rho/\rho_v)^{1/2}))(4g/C_D)^{1/4}(\sigma\Delta\rho/\rho_v^2)^{1/4}-1.4L_S \quad (11)$$

Equation 11 can be rewritten

$$C_{S,ult} = C_{S0} - 1.4\,L_S \quad (12)$$

Where C_{S0} denotes the flood capacity factor at zero liquid rate, given by

$$C_{S0} = (1.4/(1+1.4(\Delta\rho/\rho_v)^{1/2}))(4g/C_D)^{1/4}(\sigma\Delta\rho/\rho_v^2)^{1/4} \quad (13)$$

EXTENSION TO LOW LIQUID LOADS

As stated earlier, the Stupin model and correlation were shown (1, 2) to give good predictions to ultimate capacities for liquid rates of 40–140 $m^3/h\text{-}m^2$. As noted, the correlation tends to predict high at lower liquid loads.

Figure 1 is a good illustration. The correlation is shown to work well for liquid rate exceeding 35-50 $m^3/h\text{-}m^2$, but grossly overestimates data below 25 $m^3/h\text{-}m^2$. Specifically, the correlation predicts that ultimate capacity keeps increasing as the liquid load is lowered below 35-50 $m^3/h\text{-}m^2$, while the data tend to suggest that reducing the liquid load below about 35-50 $m^3/h\text{-}m^2$ does not increase ultimate capacity. It appears that once the liquid load is reduced to a certain value (in Figure 1 about 35-50 $m^3/h\text{-}m^2$), the ultimate C_S reaches a limiting value, $C_{S,\,Limit}$, at which it stays when the liquid load is reduced further.

Figure 2 is a plot of the $C_{S,\,Limit}$ values derived from experimental data for various systems plotted against C_{S0} as defined by equation 13. The open symbols (with a white background) on this figure are for systems where the highest values of C_S measured (at the lowest liquid rate measured) are still on the trend line and therefore $C_{S,\,limit}$ is greater than the data value shown. Figure 2 shows that these are very well correlated by

$$C_{S,\,Limit} = 0.8C_{S0} = (1.12/(1+1.4(\Delta\rho/\rho_v)^{1/2}))(4g/C_D)^{1/4}(\sigma\Delta\rho/\rho_v^2)^{1/4} \quad (14)$$

This will make the revised ultimate capacity factor, $C_{S,\,ult}$, the smallest of

$$C_1 = (1.4/(1+1.4(\Delta\rho/\rho_v)^{1/2}))(4g/C_D)^{1/4}(\sigma\Delta\rho/\rho_v^2)^{1/4} - 1.4L_S \quad (15a)$$

$$C_2 = (1.12/(1+1.4(\Delta\rho/\rho_v)^{1/2}))(4g/C_D)^{1/4}(\sigma\Delta\rho/\rho_v^2)^{1/4} \quad (15b)$$

$$C_{S,\,ult} = (\text{The smallest between } C_1 \text{ and } C_2) \quad (15c)$$

Equation 15 is our revised ultimate capacity (system limit) correlation.

CRITICAL LIQUID LOAD

Equation 15 states that at low liquid loads the effect of liquid load on ultimate capacity becomes insignificant. The value of liquid load at which reductions in liquid rate do not increase the ultimate capacity is called the critical liquid load. This critical liquid load can be obtained by equating equations 15a and 15b, i.e.

$$(1.4/(1+1.4(\Delta\rho/\rho_v)^{1/2}))(4g/C_D)^{1/4}(\sigma\Delta\rho/\rho_v^2)^{1/4} - 1.4L_S = (1.12/(1+1.4(\Delta\rho/\rho_v)^{1/2}))(4g/C_D)^{1/4}(\sigma\Delta\rho/\rho_v^2)^{1/4} \quad (16)$$

Giving

$$L_{S,critical} = (0.2/(1+1.4(\Delta\rho/\rho_v)^{1/2}))(4g/C_D)^{1/4}(\sigma\Delta\rho/\rho_v^2)^{1/4} \quad (17)$$

LIQUID HOLDUP AT LOW LIQUID LOADS

The fraction of liquid holdup as given by equation 10 is typically a small value, 15 % or less, in most fractionation systems, with much lower values for systems operating with low vapor densities. Further Equation 4 can offer us some insight into the value for holdup at low liquid rates.

The ultimate capacity does not continue to increase with decreasing liquid rates below the critical liquid load. According to equation 4, this behavior could be due to two factors, decreasing drop terminal velocity and/or decreasing holdup.

The first term relates to the terminal velocity of the drops and this term will decrease as the terminal velocity is lowered. This suggests that the drop diameter becomes smaller and the drops become easier to entrain. As the processes in the two phase region include both the agglomeration and breakup of drops, it is reasonable that for the average drop to be smaller at low liquid rates, the fraction of liquid in the vapor phase will also be lower than predicted by equation 10.

Indeed, if, at liquid rates lower than the $L_{S,critical,}$ equations 4 and 15b are used to predict holdup, the calculated range of feasible liquid fractions is generally lower than that predicted by equation 10. This range approaches zero as the liquid rate approaches zero. As the liquid fraction is a small value, a change in liquid volume fraction will have a large impact on the second term of equation 4 and will increase the negative liquid rate term.

We believe that both lower liquid holdup and lower terminal velocity terms contribute to the lower ultimate capacities than those predicted by equation 8 at low liquid loads.

USER-FRIENDLY EQUATION FORMAT

Using a $(4g/C_D)^{1/4}$ value of 0.445 (see Appendix), equation 15 can be rearranged to give a more user-friendly format. The units of the terms are those described in the List of Symbols. The rearranged format is equation 18.

$$C_1 = 0.445\,(1\text{-}F)\,(\sigma/\Delta\rho)^{0.25} - 1.4L_S \qquad (18a)$$

$$C_2 = 0.356\,(1\text{-}F)\,(\sigma/\Delta\rho)^{0.25} \qquad (18b)$$

$$C_{S,\,ult} = (\text{the smallest between } C_1 \text{ and } C_2) \qquad (18c)$$

The value of F is given by equation 10.

COMPARISON TO DATA

Figures 3-23 compare predictions from equation 15 to ultimate capacity data measured by FRI. The data bank is FRI's test data obtained in a 4-ft ID tower. Test data are present for the following devices:

1) Dual flow trays, open areas 29% of the active area, 12 mm holes, at 1.22, 1.83 and 2.44 meter tray spacing.

2) Sieve trays, sloped downcomers, 30%/7% downcomer top/bottom areas, 0.914 meter tray spacing, 12.7 mm holes, hole area 8.3% of active area, outlet weir height and clearance under downcomer 50 mm.

3) Segmental baffle trays at 0.61 m spacing, no outlet weirs and no perforations, with open areas 44% and 59% of tower cross section area.

4) 3.5 inch Pall rings

5) Commercial grid packing

6) Commercial structured packing, 100-150 m^2/m^3 specific surface area.

7) 2.5 inch Nutter rings.

The tray data (items 1-3 above) have been released by FRI and are available through the Special Collection Sections of Oklahoma State University Library, Stillwater, Oklahoma. The packing data in items 4-6 are those published in FRI's paper (1), some without giving detailed information. The packing data in item 7 were published in reference 6.

The flood point values used for packings in our work are not the same as those used in FRI's paper (1). In personal communication with FRI (7) we verified that the flood points reported by FRI for these packings are the point of hydraulic inoperability. The flood definition used by us is a multi-symptom definition of incipient flood, proposed by Bravo and Fair (8) and Billet (9), "a region of rapidly increasing pressure drop with simultaneous loss of mass transfer efficiency. Heavy entrainment is also recognized as a symptom of this region." This definition has been endorsed here and in Kister's "Distillation Design" (10), because it provides a good representation of incipient flooding which limits most commercial columns.

Figures 3-23 show excellent agreement between predictions from Equation 15 and experimental data. We could not have hoped for a closer agreement, which demonstrates the validity of our approach.

COMMERCIAL APPLICATIONS

The model presented in this paper is based on a dispersed liquid phase falling through an ascending vapor phase. In reality, many fractionation devices do not approach this concept in their mode of operation. It is not unreasonable to consider alternate configurations that separate the downflowing liquid from upflowing vapor and achieve higher capacities. However, as the devices discussed in this paper are for a specific commercial application to achieve intimate contact between the phases and fractional distillation of the components, we consider only devices and flow configurations that provide for this intimate contact. Therefore, the concept of ultimate capacity applies to devices that include intimate vapor and liquid contact. The authors are aware of operations where the flows in columns are not uniform and the overall result is operations at a capacity above the ultimate capacity. For instance, an operation with the liquid flowing down one side of the tower and the vapor flowing up the other side with minimal contact. As the contacting efficiency for this situation is low, this countercurrent flow situation would not be considered as covered by the ultimate capacity.

Distillation trays commonly include downcomers to convey the liquid down the tower. While this avoids the requirement to force the liquid down the tower as a dispersed phase which is fighting the up flowing vapor, it takes space in the tower for downcomers and requires zones for the separation of the two phases. The net effect of the gain from eliminating the countercurrent flow of the dispersed liquid phase in the vapor space is offset by the reduced flow area for the vapor.

The data published by FRI and other data included in the literature show that dual flow trays and other high open area counterflow devices operate at throughputs that can be only approached by trays with downcomers. Generally devices other than dual flow trays include surfaces which impede the downward flow of the liquid to some extent and therefore have reduced capacities.

Equation 7 and subsequent equations of this paper include the acceleration of gravity. This acceleration provides the driving force for separation and downward flow of the liquid. Therefore, we would expect the ultimate capacity to be lower on the moon, but higher on Mars. The ultimate capacity as discussed in this paper provides a limit or target in capacity that we should consider for what is achievable in columns based on gravity for providing the force for the separation and downward flow of the liquid.

Not many plants operate dualflow trays at 2.44 meter tray spacing. On the other hand, commercial grid, structured packings of 100-150 m^2/m^3 specific surface area or less,
3-inch modern random packings, and baffle trays at 0.6 meters spacing and an open area of 50% are common in commercial practice. Our work shows that these high-capacity devices often approach the system limit. Even conventional trays at 0.91 meters spacings, like the sieve trays used here, can under some conditions approach the system limit.

Once a device reaches the system limit, its capacity can not be improved any further. Replacement by an alternative more open device will do little to increase capacity. That is because once a device reaches the system limit, its capacity is controlled by the droplet settling velocity in the intertray space or in the packing interstices.

The only device capable of debottlenecking a tray system limit device is one that introduces a new force that helps disentrain the vapor space. Manning (14) foresaw that increasing the gravity force will help with drop settling. New-millennium trays such as Koch-Glitsch's Ultrafrac or Shell Global's Consep use a cyclone principle to enhance disentrainment and can potentially increase the capacity beyond the system limit. Even the horizontal vapor push in trays like ExxonMobil's jet tray, Koch Glitsch's Nye and Max-Frac trays, Sulzer's MVGT tray or UOP's ECMD tray can help settle the entrained drops, but to a much lesser degree. It is unknown whether these devices can actually exceed the system limit.

There have been some reports (e.g., 11) of towers operating at capacity factors well in excess of the system limit. It is unknown how accurate these reports are, but some of it is quite conceivable. We have seen many towers operated partially flooded, but in a stable condition. There will be sections operating at excess entrainment, excess pressure drop and low efficiency, but this may be acceptable if there is an excess of stages, or the separation is not critical. Our experience has been that direct contact heat transfer sections in refinery fractionators ("pumparounds") occasionally operate partially flooded and achieve satisfactory heat transfer. In these sections, vapor loads rapidly diminishes as one ascends the section, so the flooding may remain local and not propagate and destabilize the tower.

The examples cited in the above paragraph, however, are exceptions rather than the rule. In most cases the system limit is a severe limit that cannot be exceeded and will define the ultimate capacity of a fractionator.

CONCLUSION

The Ultimate Capacity is a useful concept and represents the limiting vapor velocity independent of tray parameters. This paper extends the earlier correlation of Stupin to lower liquid rates. This correlation provides a useful means to check the limiting capacity that could be expected for a given column diameter and set targets for the capacities of new devices. The challenge is to develop devices that exceed this capacity limit. Devices which use cyclones to separate the liquid from the vapor can possibly exceed this limit.

ACKNOWLEDGEMENT

The contribution of Sam Alsheikh from Fluor Daniel's Aliso Viejo office is gratefully appreciated and acknowledged.

LIST OF SYMBOLS

C_D	drag coefficient, defined in equation 1
$C_{S,\,ult}$	capacity factor at ultimate capacity, $V_{S,\,ult}\left(\frac{\rho_V}{\Delta\rho}\right)^{1/2}$, m/s
C_{S0}	flood capacity factor at zero liquid load per Stupin's 1965 correlation (4), defined by equation 13, m/s
$C_{S,\,limit}$	The highest capacity factor obtained when liquid load is reduced, m/s.
C_1, C_2	parameters defined by equation 15, m/s
F	fraction of volume occupied by the liquid phase
g	acceleration of gravity, m/sec2
h	thickness of a flattened drop
L_a	actual liquid velocity, m/sec
L_S	liquid velocity based on the superficial area, m/sec
$L_{S,\,critical}$	The liquid load at which reducing the liquid load no longer increases the ultimate capacity, m/s.
Δp	pressure difference
S	frontal area of a drop
Δu	terminal velocity of a drop, m/sec
V	volume of a drop
V_a	actual vapor velocity, m/sec
V_S	vapor velocity based on superficial area, m/sec
$V_{S,\,ult}$	limiting vapor velocity or vapor velocity at ultimate capacity based on the superficial area, m/sec
ρ_L	liquid density, kg/m3
ρ_V	vapor density, kg/m3
$\Delta\rho$	$(\rho_L - \rho_V)$, kg/m^3
σ	surface tension, dynes/cm

REFERENCES

1. Fitz, C.W., and Kunesh, J.G., “System Limit or Ultimate Capacity”, paper presented at the Distillation Topical Symposium, AIChE Spring Meeting, Houston, Texas, April 2001.

2. Tek, R., F.R.I. Topical Reports 21 (1959) and 25 (1961). Available through Special Collections Section, Oklahoma State University Library, Stillwater, Oklahoma.

3. Hachmuth, K. E. Private Communication, 1963. See reference (4).

4. Stupin, W.J., F.R.I. Topical report 34, 1965. Available through Special Collections Section, Oklahoma State University Library, Stillwater, Oklahoma.

5. Levich, V.G., “Physicochemical Hydrodynamics”, (Translated by Scripta Techinca, Inc.), Prentice Hall, N. J., 1962, pages 429-432.

6. Nutter, D.E., Silvey, F.C., Stober, B.K., I.Chem.E.Symp. Ser. 128, p. A99, 1992.

7. Kunesh, J.G., Private Communication, December 19, 2001.

8. Fair, J.R., and Bravo, J.L., I.Chem.E.Symp.Ser. 104, p. A183, 1987.

9. Billet, R., “Distillation Engineering”, Chemical Publishing Co., New York, 1979.

10. Kister, H.Z., “Distillation Design”, McGraw-Hill, NY, 1992.

11. Hanson, D.W., Lieberman, N.P., and Lieberman, E.T., Hydroc. Proc., p. 55, July 1999.

12. Souders, M.Jr., and Brown, G. G., Ind. Eng. Chem., 26(1), p.98, 1934.

13. Stichlmair, J., Grundlagen der Dimensionierung des Gas/Flüssigkeit-Kontaktapparates, Bodenkolonne, Verlag Chemie, Weinheim, New York, 1978.

14. Manning, E.M. Jr., I&EC 56 (4), p. 14, 1964.

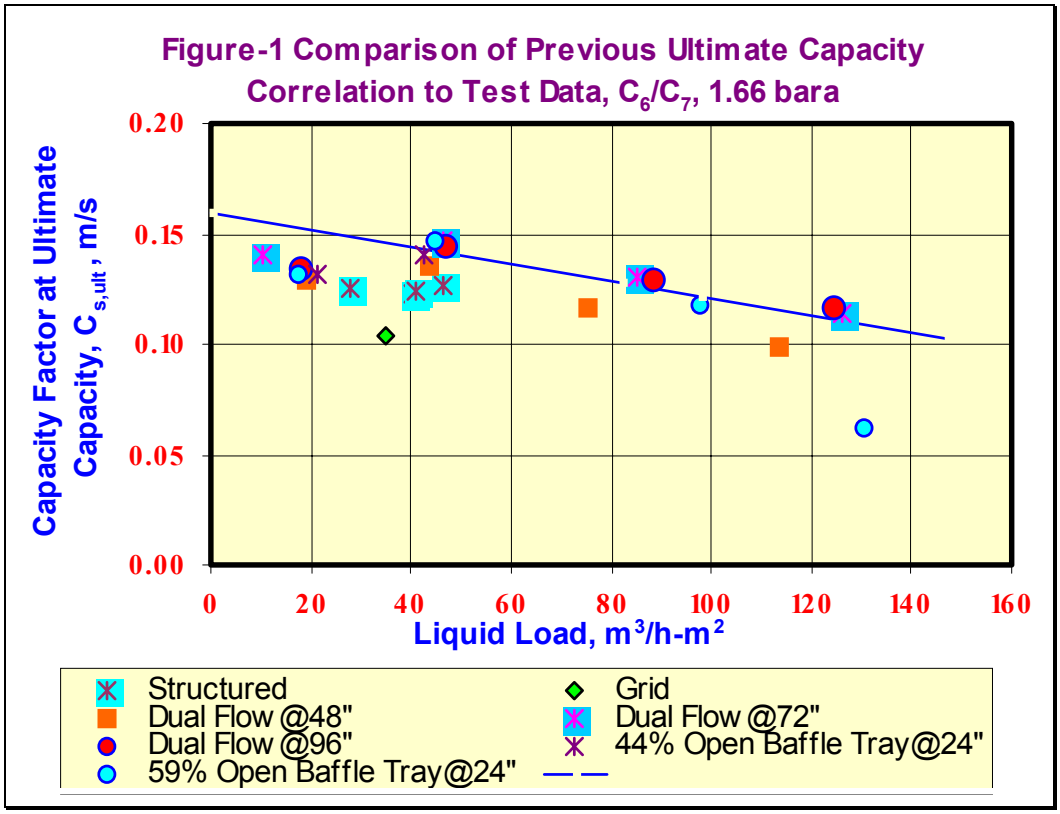
Figure-1 Comparison of Previous Ultimate Capacity Correlation to Test Data, C_6/C_7, 1.66 bara
Capacity Factor at Ultimate Capacity, $C_{s,ult}$, m/s
0.20
0.15
0.10
0.05
0.00
0
20
40
60
80
100
120
140
160
Liquid Load, $m^3/h\text{-}m^2$
Structured
Dual Flow @48"
Dual Flow @96"
59% Open Baffle Tray@24"
Grid
Dual Flow @72"
44% Open Baffle Tray@24"

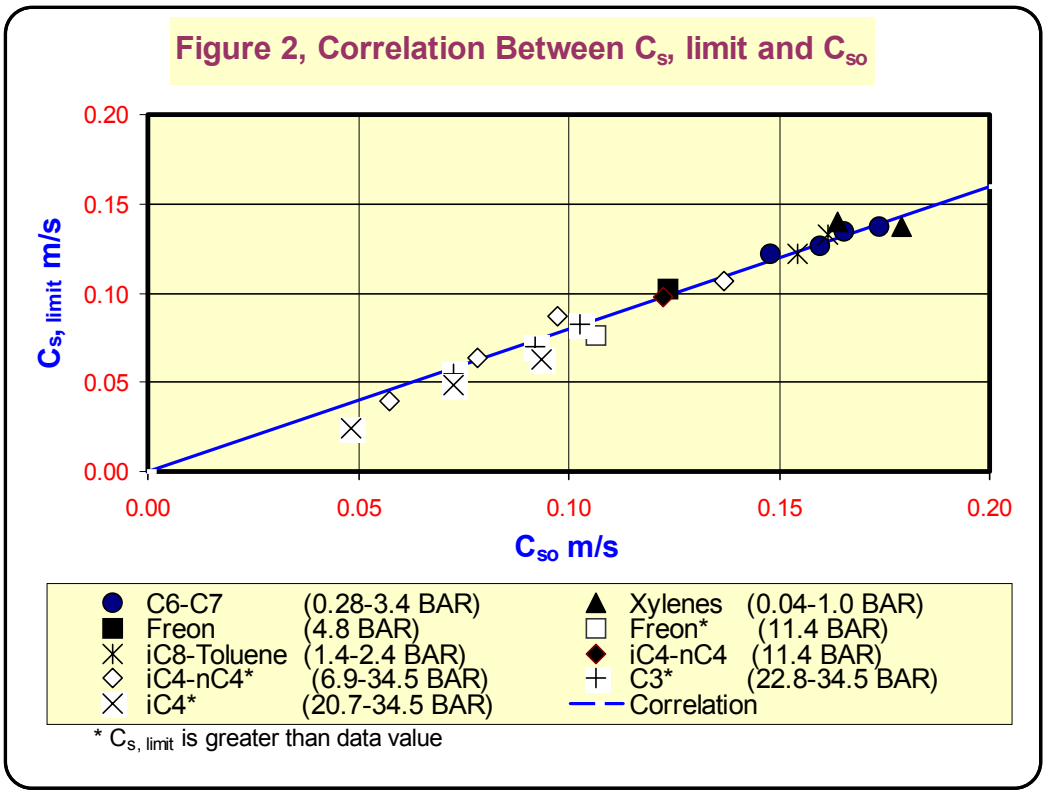
Figure 2, Correlation Between C_s, limit and C_{so}
$C_{s,\ limit}$ m/s
0.20
0.15
0.10
0.05
0.00
0.00
0.05
0.10
0.15
0.20
C_{so} m/s
C6-C7 (0.28-3.4 BAR)
Freon (4.8 BAR)
iC8-Toluene (1.4-2.4 BAR)
iC4-nC4* (6.9-34.5 BAR)
iC4* (20.7-34.5 BAR)
Xylenes (0.04-1.0 BAR)
Freon* (11.4 BAR)
iC4-nC4 (11.4 BAR)
C3* (22.8-34.5 BAR)
Correlation
* $C_{s,\ limit}$ is greater than data value

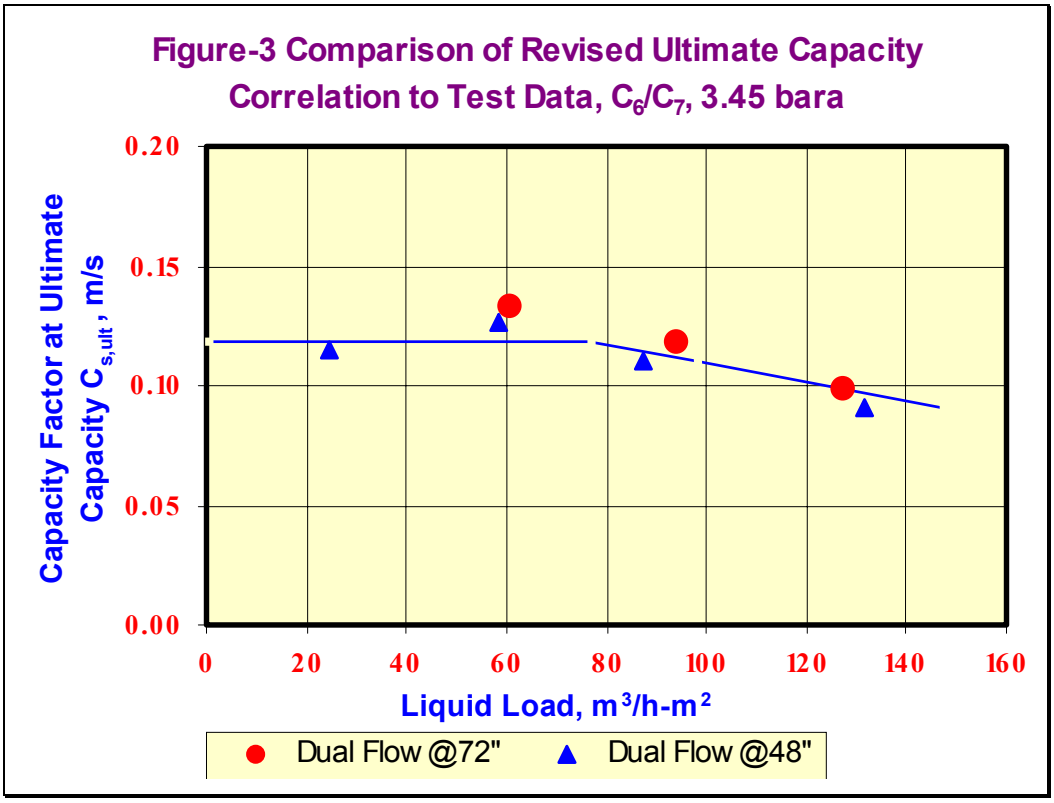
Figure-3 Comparison of Revised Ultimate Capacity
Correlation to Test Data, C6/C7, 3.45 bara
Capacity Factor at Ultimate Capacity Cs,ult , m/s
0.20
0.15
0.10
0.05
0.00
0
20
40
60
80
100
120
140
160
Liquid Load, m3/h-m2
Dual Flow @72"
Dual Flow @48"

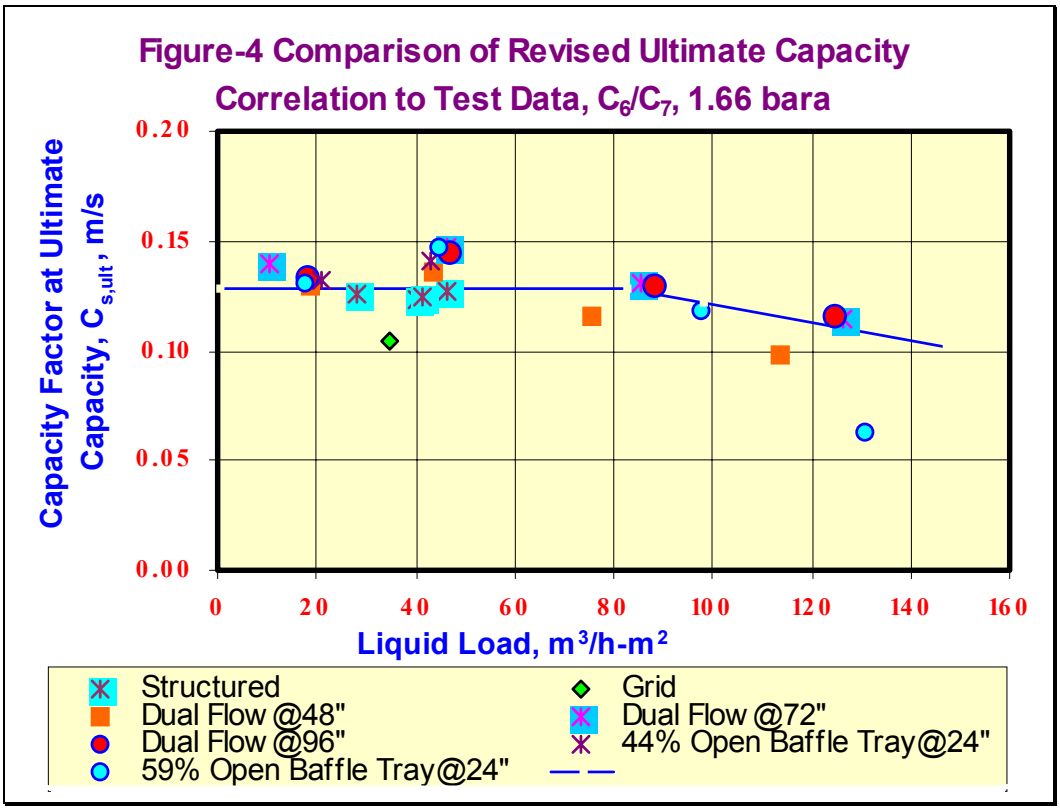
Figure-4 Comparison of Revised Ultimate Capacity
Correlation to Test Data, C6/C7, 1.66 bara
Capacity Factor at Ultimate Capacity, Cs,ult , m/s
0.20
0.15
0.10
0.05
0.00
0
20
40
60
80
100
120
140
160
Liquid Load, m3/h-m2
Structured
Dual Flow @48"
Dual Flow @96"
59% Open Baffle Tray@24"
Grid
Dual Flow @72"
44% Open Baffle Tray@24"

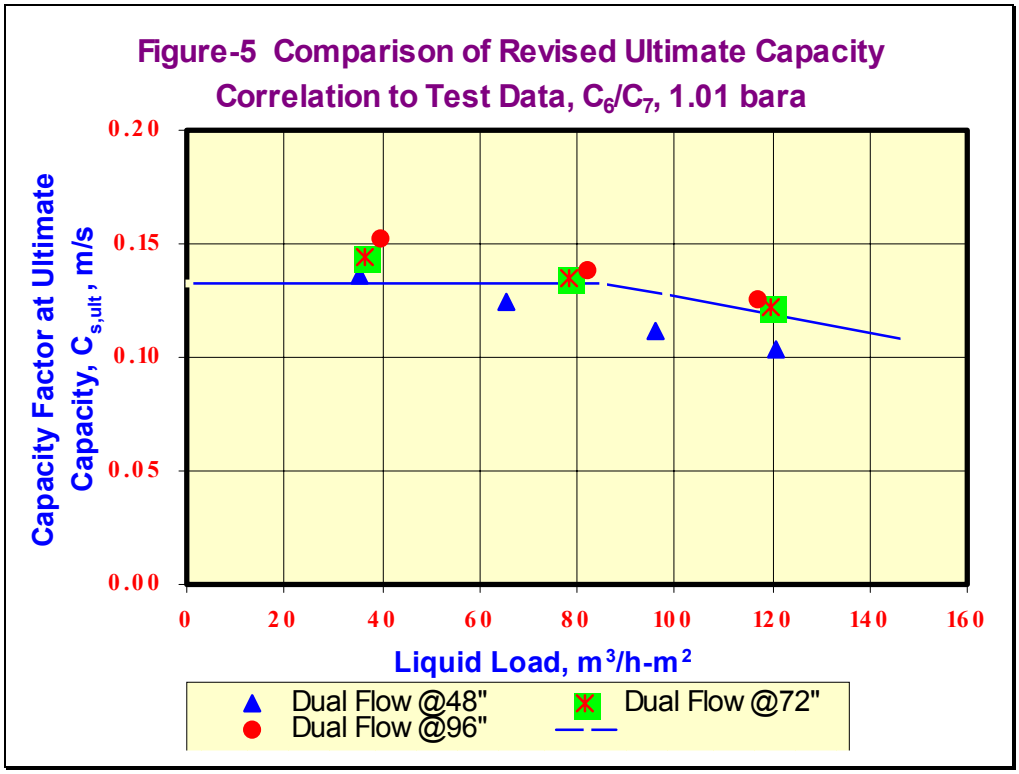
Figure-5 Comparison of Revised Ultimate Capacity
Correlation to Test Data, C6/C7, 1.01 bara
Capacity Factor at Ultimate Capacity, Cs,ult, m/s
0.20
0.15
0.10
0.05
0.00
0
20
40
60
80
100
120
140
160
Liquid Load, m3/h-m2
Dual Flow @48"
Dual Flow @96"
Dual Flow @72"

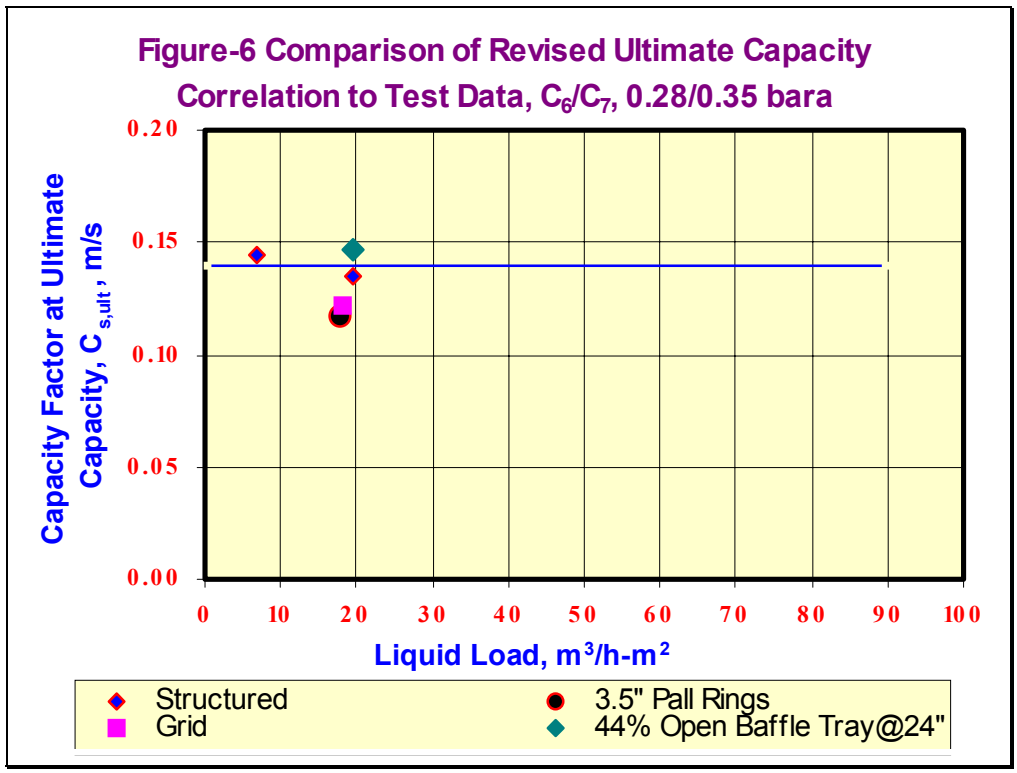
Figure-6 Comparison of Revised Ultimate Capacity
Correlation to Test Data, C6/C7, 0.28/0.35 bara
Capacity Factor at Ultimate Capacity, Cs,ult, m/s
0.20
0.15
0.10
0.05
0.00
0
10
20
30
40
50
60
70
80
90
100
Liquid Load, m3/h-m2
Structured
Grid
3.5" Pall Rings
44% Open Baffle Tray@24"

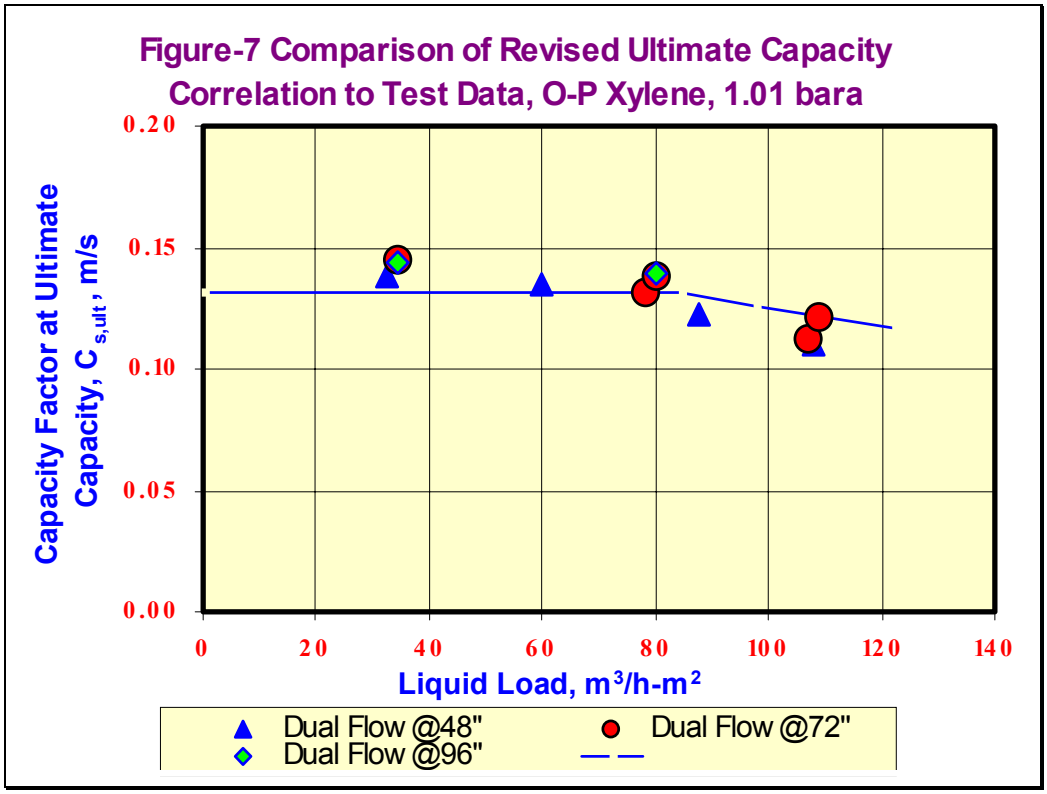
Figure-7 Comparison of Revised Ultimate Capacity Correlation to Test Data, O-P Xylene, 1.01 bara
Capacity Factor at Ultimate Capacity, $C_{s,ult}$, m/s
0.20
0.15
0.10
0.05
0.00
0
20
40
60
80
100
120
140
Liquid Load, $m^3/h\text{-}m^2$
Dual Flow @48"
Dual Flow @96"
Dual Flow @72"

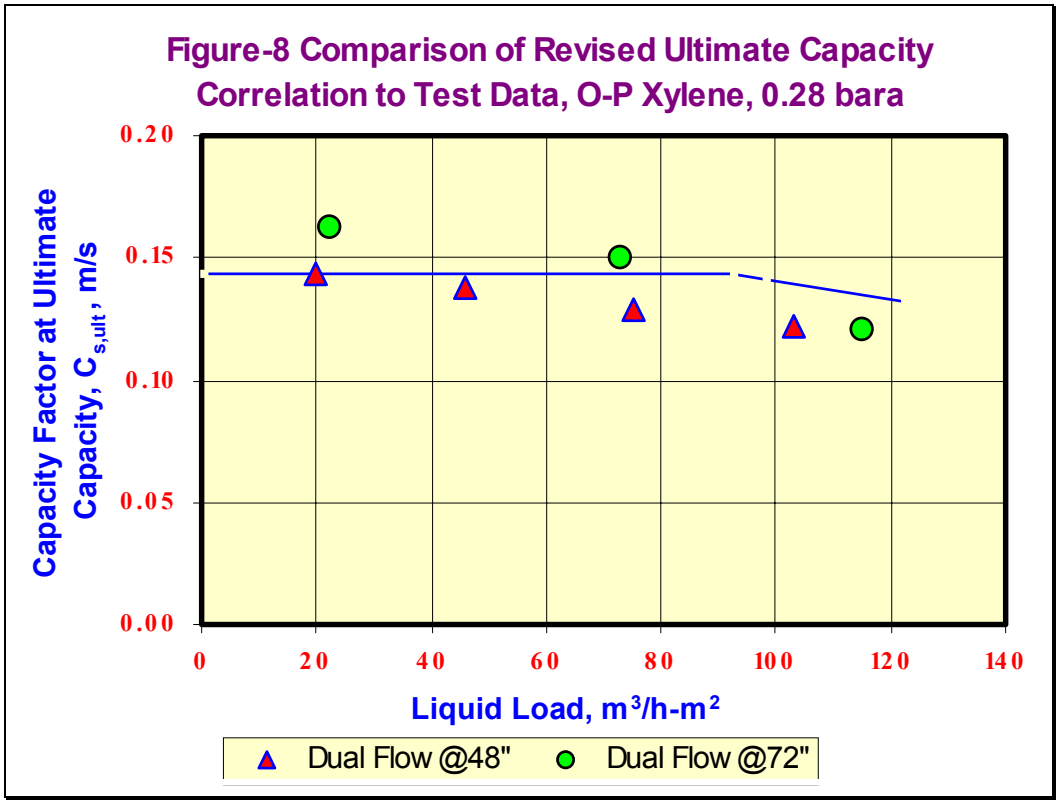
Figure-8 Comparison of Revised Ultimate Capacity Correlation to Test Data, O-P Xylene, 0.28 bara
Capacity Factor at Ultimate Capacity, $C_{s,ult}$, m/s
0.20
0.15
0.10
0.05
0.00
0
20
40
60
80
100
120
140
Liquid Load, $m^3/h\text{-}m^2$
Dual Flow @48"
Dual Flow @72"

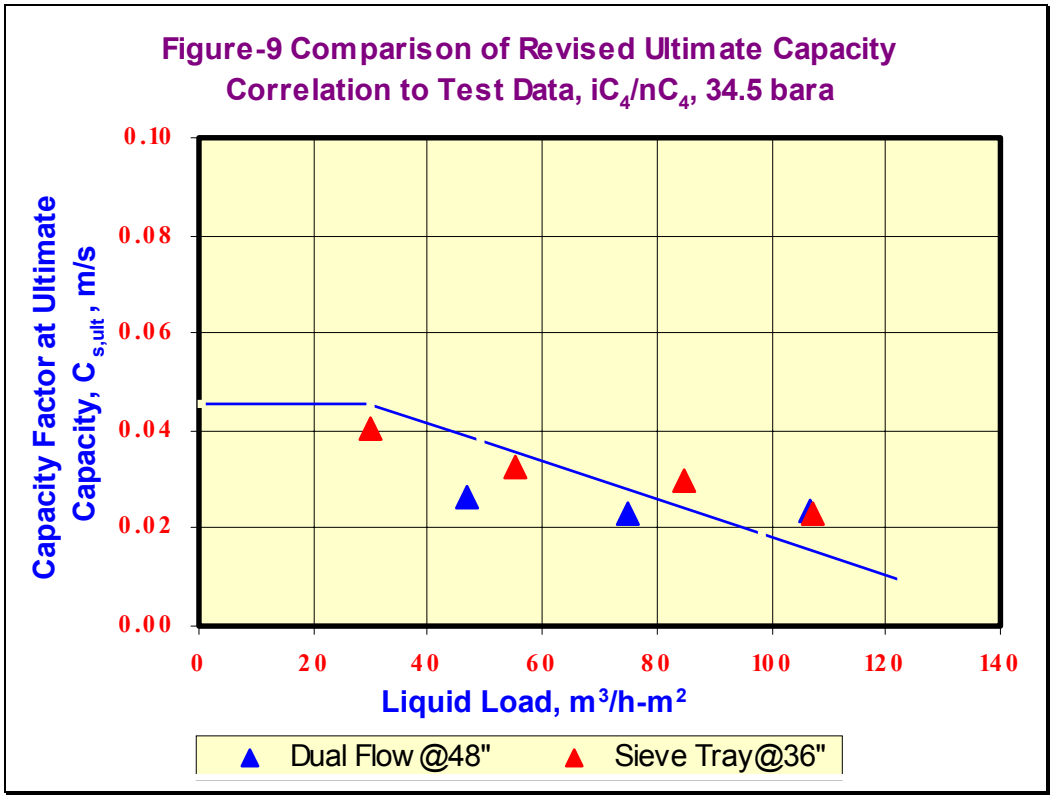
Figure-9 Comparison of Revised Ultimate Capacity Correlation to Test Data, iC4/nC4, 34.5 bara
Capacity Factor at Ultimate Capacity, Cs,ult, m/s
0.10
0.08
0.06
0.04
0.02
0.00
0
20
40
60
80
100
120
140
Liquid Load, m3/h-m2
Dual Flow @48"
Sieve Tray@36"

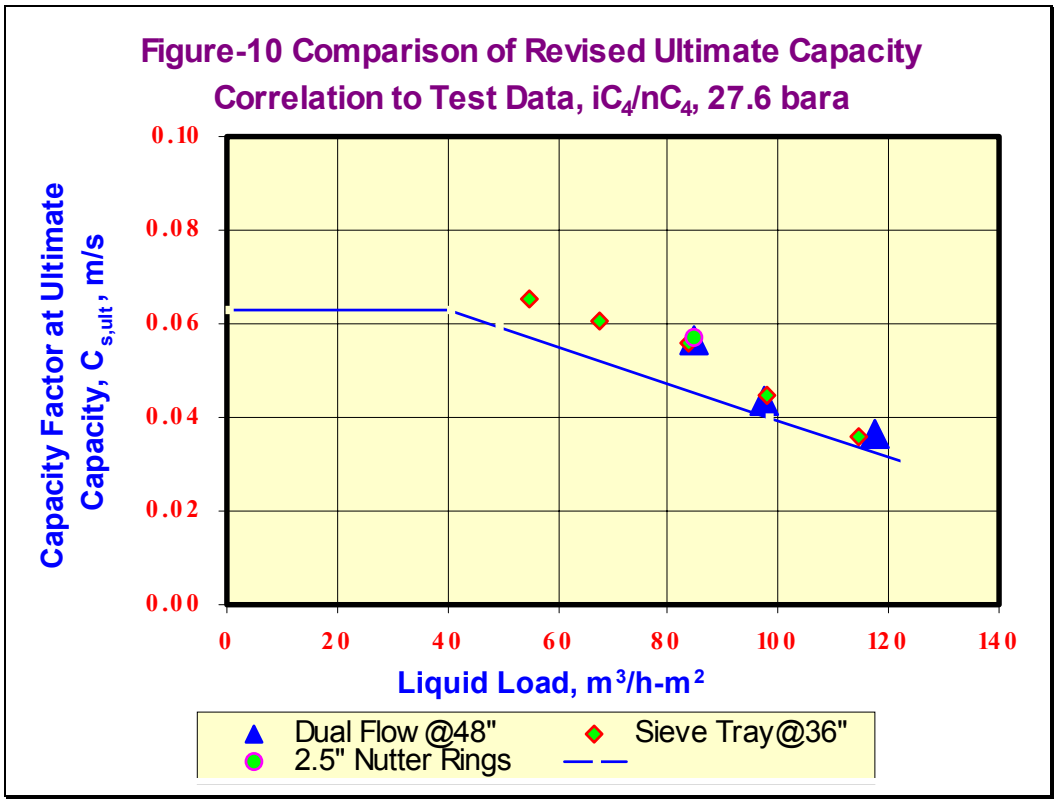
Figure-10 Comparison of Revised Ultimate Capacity Correlation to Test Data, iC4/nC4, 27.6 bara
Capacity Factor at Ultimate Capacity, Cs,ult, m/s
0.10
0.08
0.06
0.04
0.02
0.00
0
20
40
60
80
100
120
140
Liquid Load, m3/h-m2
Dual Flow @48"
Sieve Tray@36"
2.5" Nutter Rings

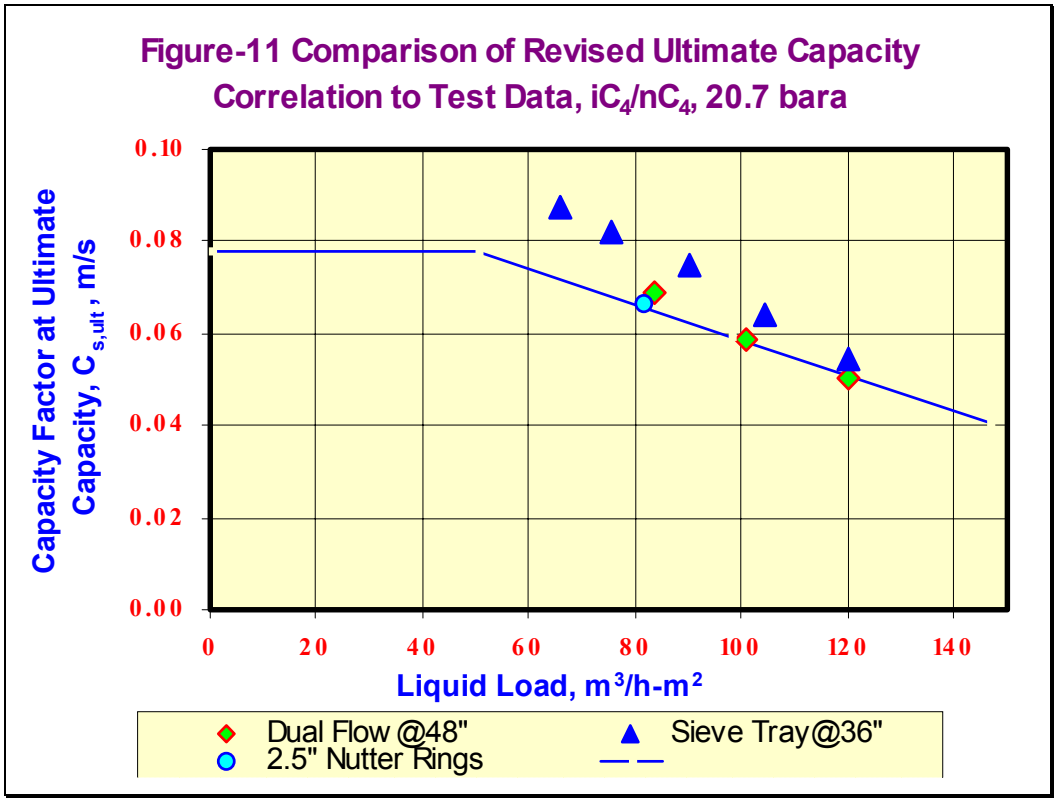
Figure-11 Comparison of Revised Ultimate Capacity Correlation to Test Data, iC4/nC4, 20.7 bara
Capacity Factor at Ultimate Capacity, Cs,ult, m/s
0.10
0.08
0.06
0.04
0.02
0.00
0
20
40
60
80
100
120
140
Liquid Load, m3/h-m2
Dual Flow @48"
Sieve Tray@36"
2.5" Nutter Rings

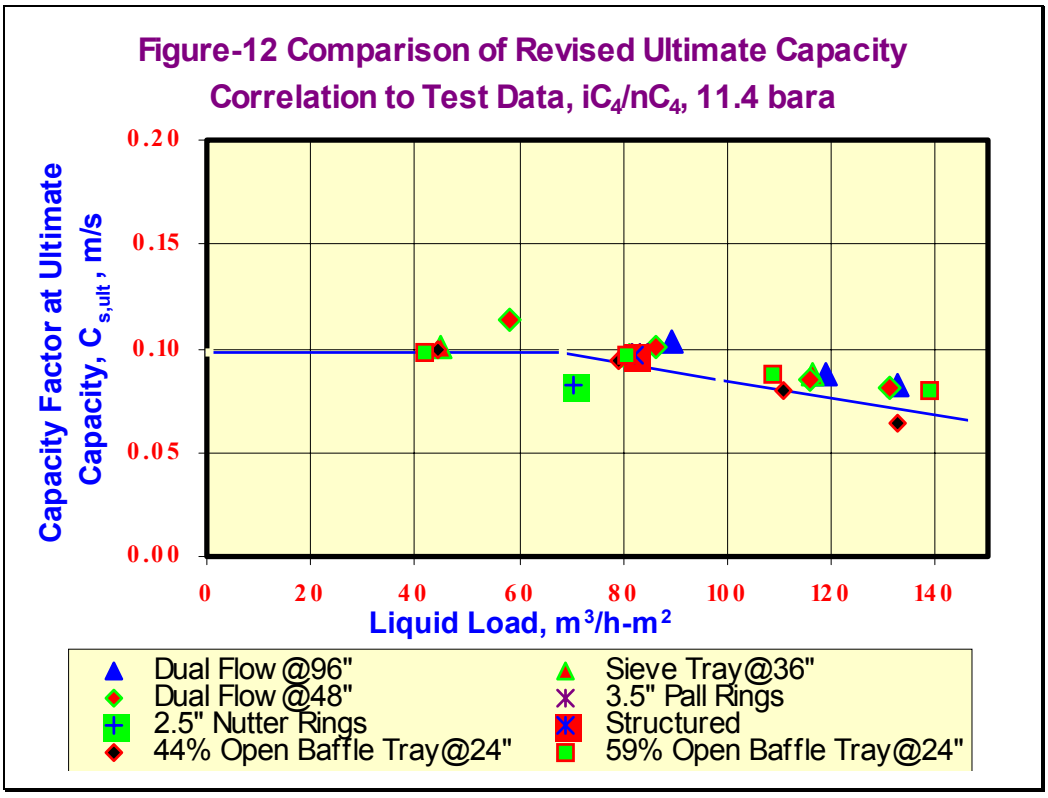
Figure-12 Comparison of Revised Ultimate Capacity Correlation to Test Data, iC4/nC4, 11.4 bara
Capacity Factor at Ultimate Capacity, Cs,ult, m/s
0.20
0.15
0.10
0.05
0.00
0
20
40
60
80
100
120
140
Liquid Load, m3/h-m2
Dual Flow @96"
Dual Flow @48"
2.5" Nutter Rings
44% Open Baffle Tray@24"
Sieve Tray@36"
3.5" Pall Rings
Structured
59% Open Baffle Tray@24"

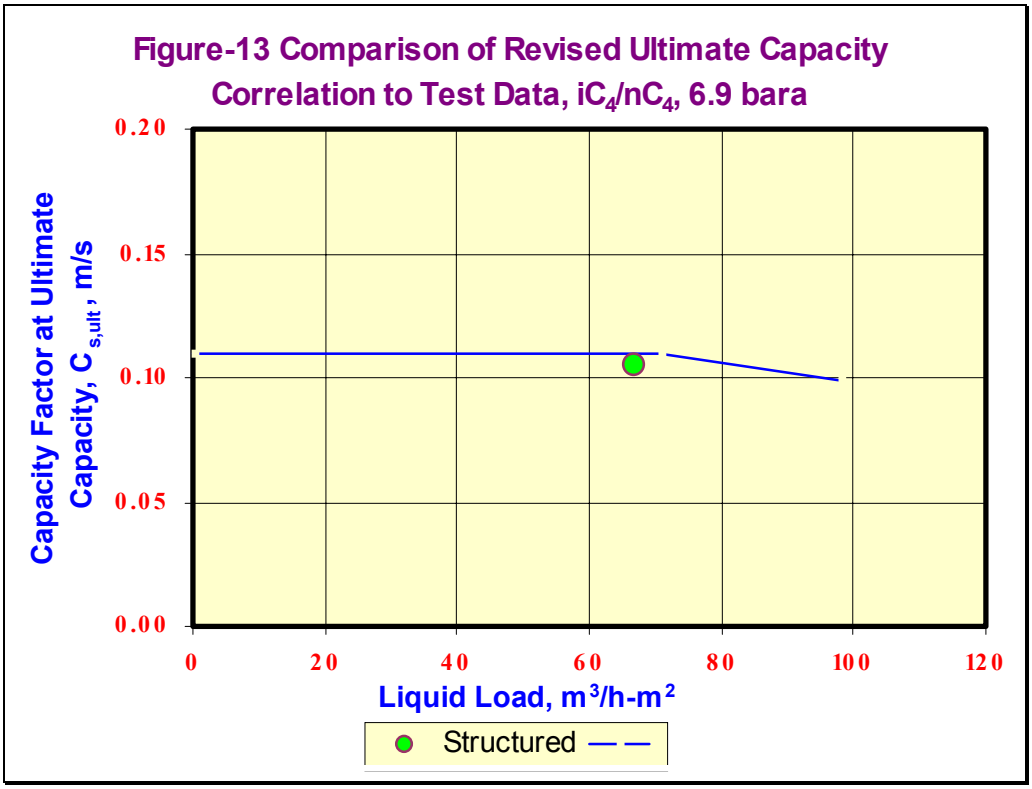
Figure-13 Comparison of Revised Ultimate Capacity
Correlation to Test Data, iC4/nC4, 6.9 bara
Capacity Factor at Ultimate Capacity, Cs,ult, m/s
0.20
0.15
0.10
0.05
0.00
0
20
40
60
80
100
120
Liquid Load, m3/h-m2
Structured

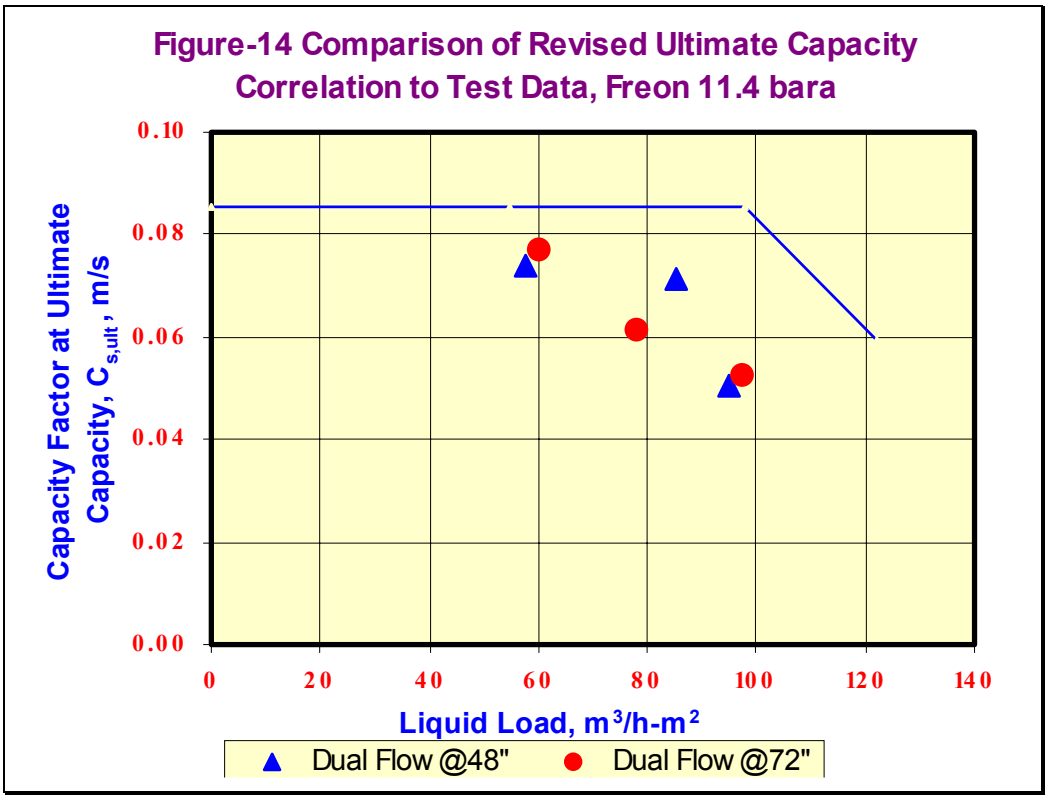
Figure-14 Comparison of Revised Ultimate Capacity
Correlation to Test Data, Freon 11.4 bara
Capacity Factor at Ultimate Capacity, Cs,ult, m/s
0.10
0.08
0.06
0.04
0.02
0.00
0
20
40
60
80
100
120
140
Liquid Load, m3/h-m2
Dual Flow @48"
Dual Flow @72"

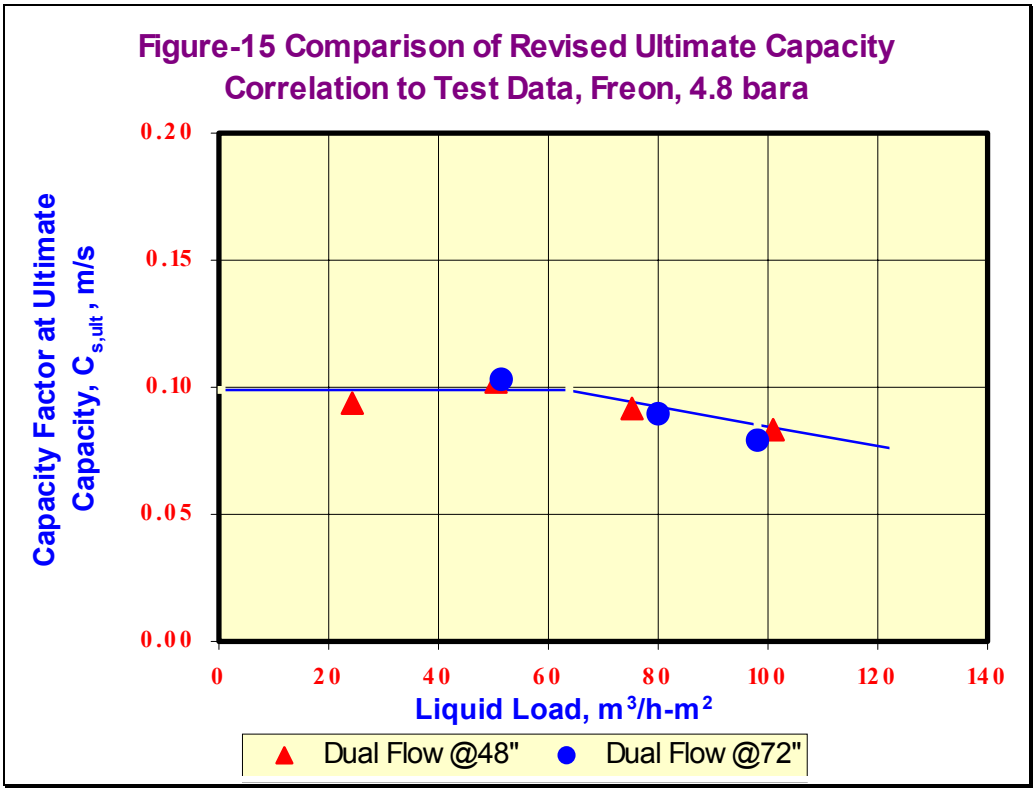
Figure-15 Comparison of Revised Ultimate Capacity
Correlation to Test Data, Freon, 4.8 bara
Capacity Factor at Ultimate Capacity, $C_{s,ult}$, m/s
0.20
0.15
0.10
0.05
0.00
0
20
40
60
80
100
120
140
Liquid Load, $m^3/h\text{-}m^2$
Dual Flow @48"
Dual Flow @72"

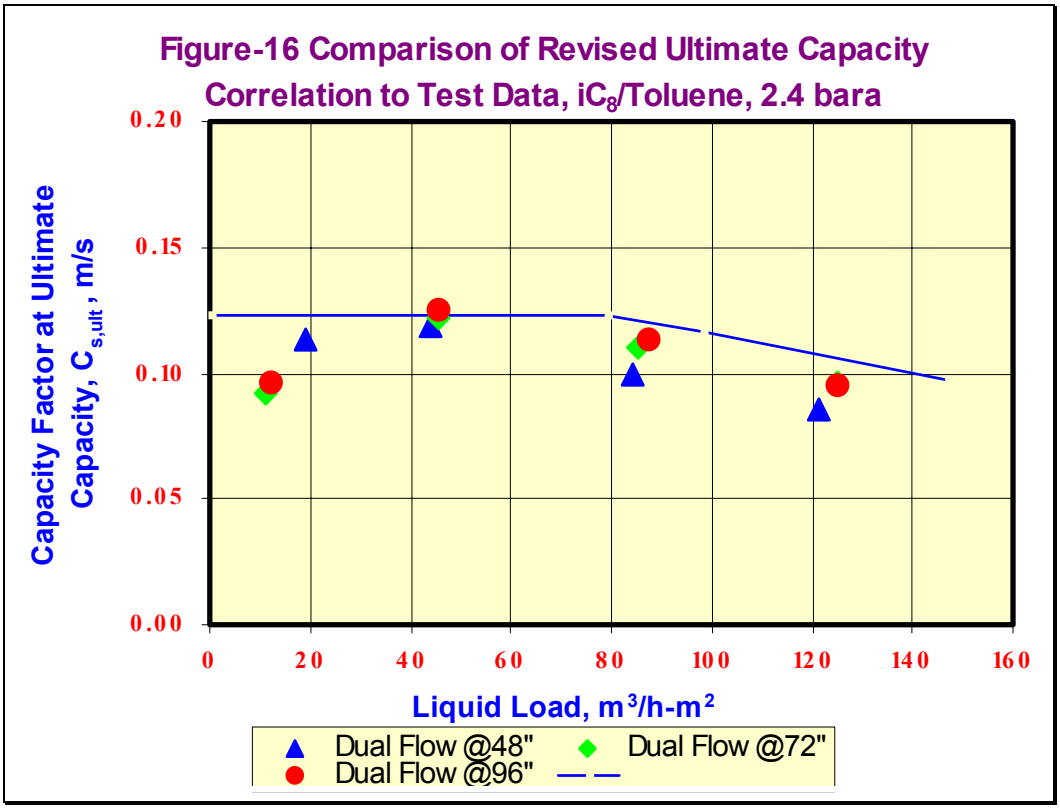
Figure-16 Comparison of Revised Ultimate Capacity
Correlation to Test Data, iC_8/Toluene, 2.4 bara
Capacity Factor at Ultimate Capacity, $C_{s,ult}$, m/s
0.20
0.15
0.10
0.05
0.00
0
20
40
60
80
100
120
140
160
Liquid Load, $m^3/h\text{-}m^2$
Dual Flow @48"
Dual Flow @72"
Dual Flow @96"

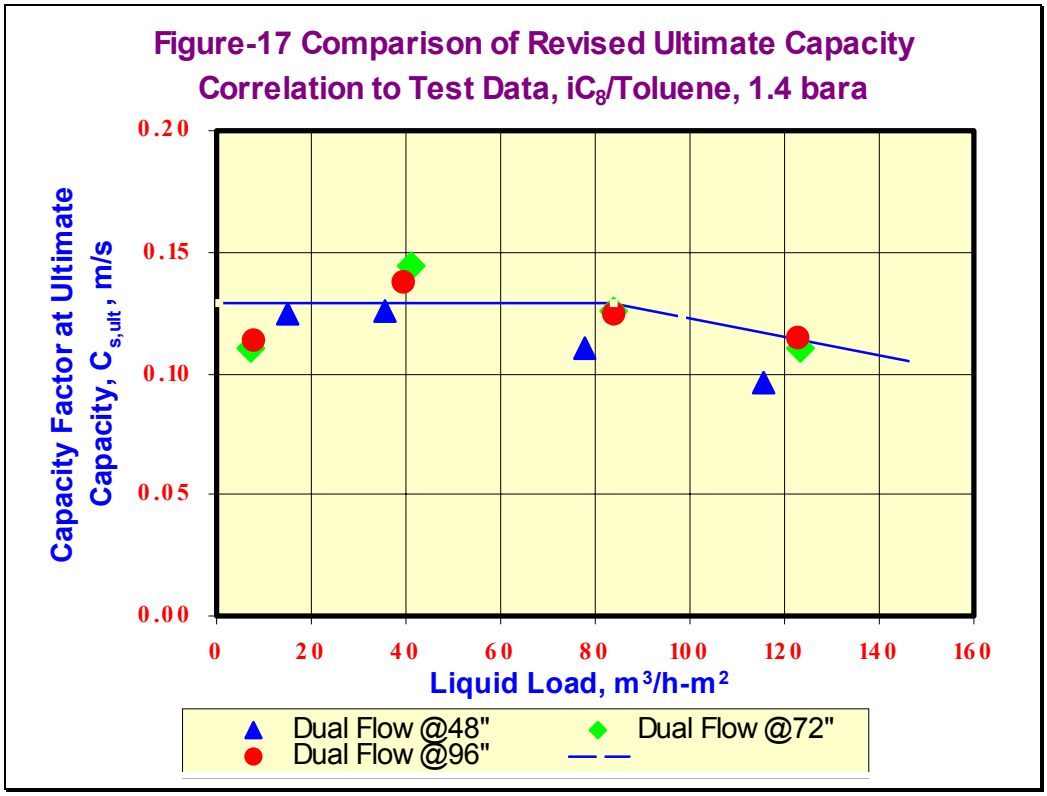
Figure-17 Comparison of Revised Ultimate Capacity Correlation to Test Data, iC8/Toluene, 1.4 bara
Capacity Factor at Ultimate Capacity, Cs,ult, m/s
0.20
0.15
0.10
0.05
0.00
0
20
40
60
80
100
120
140
160
Liquid Load, m3/h-m2
Dual Flow @48"
Dual Flow @72"
Dual Flow @96"

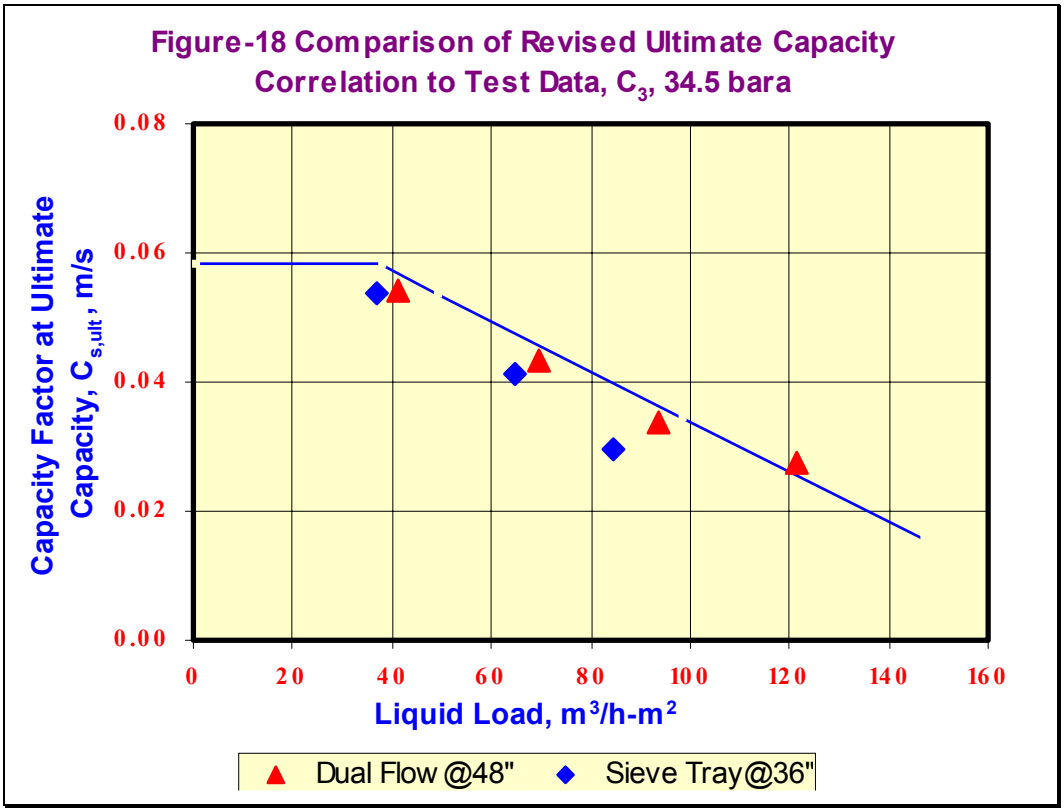
Figure-18 Comparison of Revised Ultimate Capacity Correlation to Test Data, C3, 34.5 bara
Capacity Factor at Ultimate Capacity, Cs,ult, m/s
0.08
0.06
0.04
0.02
0.00
0
20
40
60
80
100
120
140
160
Liquid Load, m3/h-m2
Dual Flow @48"
Sieve Tray@36"

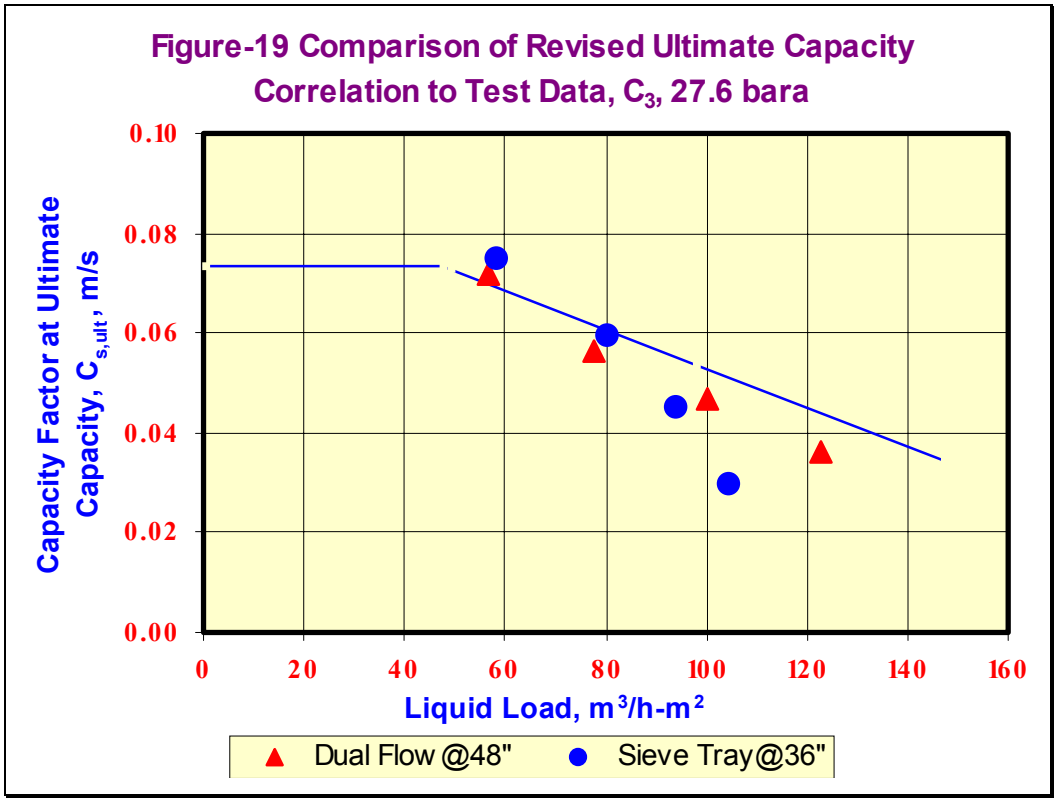
Figure-19 Comparison of Revised Ultimate Capacity Correlation to Test Data, C_3, 27.6 bara
Capacity Factor at Ultimate Capacity, $C_{s,ult}$, m/s
0.10
0.08
0.06
0.04
0.02
0.00
0
20
40
60
80
100
120
140
160
Liquid Load, $m^3/h\text{-}m^2$
Dual Flow @48"
Sieve Tray@36"

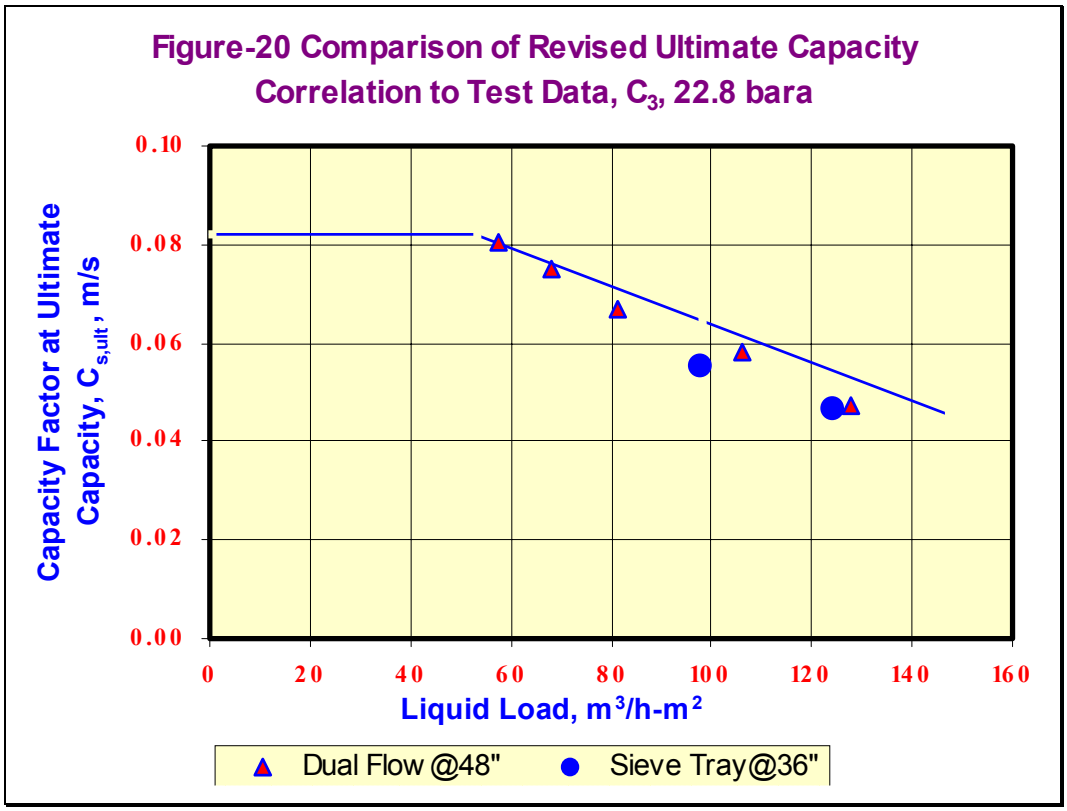
Figure-20 Comparison of Revised Ultimate Capacity Correlation to Test Data, C_3, 22.8 bara
Capacity Factor at Ultimate Capacity, $C_{s,ult}$, m/s
0.10
0.08
0.06
0.04
0.02
0.00
0
20
40
60
80
100
120
140
160
Liquid Load, $m^3/h\text{-}m^2$
Dual Flow @48"
Sieve Tray@36"

Figure-21 Comparison of Revised Ultimate Capacity Correlation to Test Data, iC_4, 34.5 bara

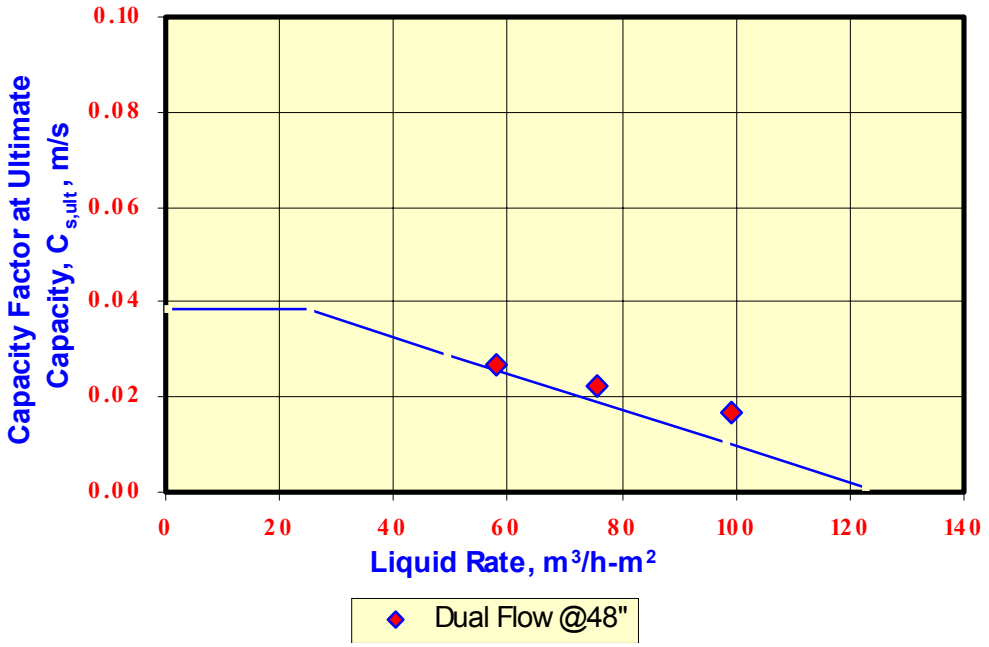

Figure-22 Comparison of Revised Ultimate Capacity Correlation to Test Data, iC_4, 20.7 bara

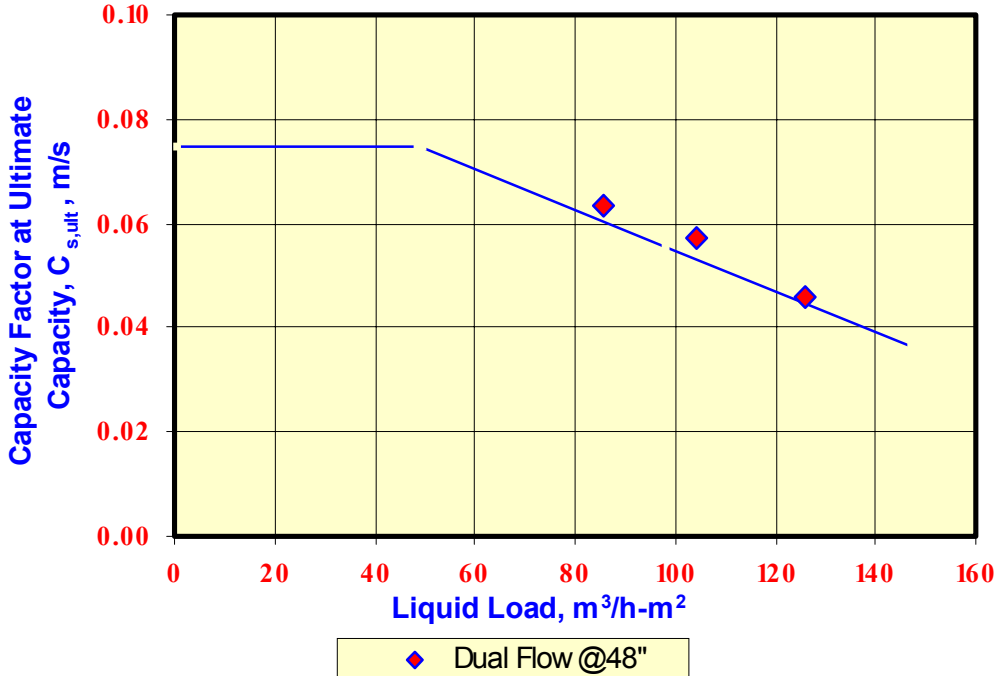

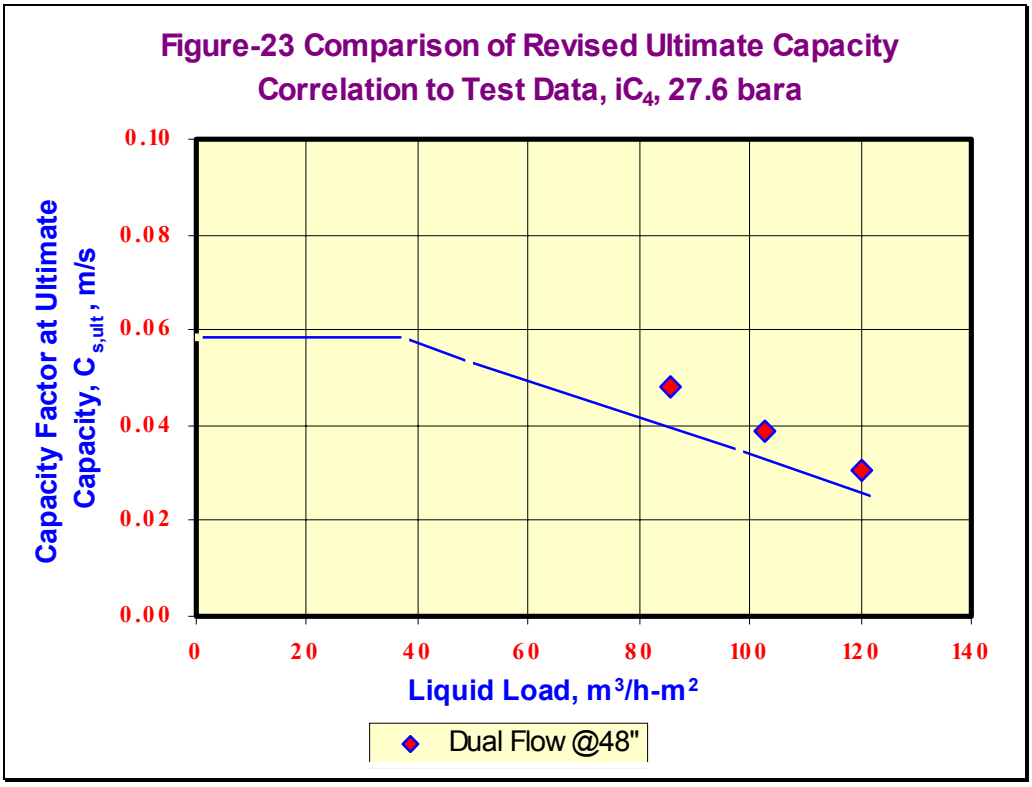
Figure-23 Comparison of Revised Ultimate Capacity
Correlation to Test Data, iC4, 27.6 bara
Capacity Factor at Ultimate Capacity, Cs,ult, m/s
0.10
0.08
0.06
0.04
0.02
0.00
0
20
40
60
80
100
120
140
Liquid Load, m3/h-m2
Dual Flow @48"

APPENDIX

Limiting or Terminal Velocity of Large Single Drops

Equating the force of gravity in a drop to the drag induces by the relative velocity between the drop and the vapor, we have

$$\Delta\rho\, g\, V = C_D\, \rho_V\, \frac{(\Delta u)^2}{2}\, S \tag{1}$$

where Δu = terminal velocity of the drop

Levich (5) presents the following derivation to describe the limiting velocity of drops as they become large. For large drops the terminal velocity is relatively independent of drop diameter. As the volume of the drop increases, the drop flattens out and the frontal area increases, increasing the hydrodynamic resistance. Considering a flattened drop falling at the terminal velocity, the pressure difference upstream and downstream of the drop is:

$$\Delta p = \rho_V \frac{(\Delta u)^2}{2} \tag{2}$$

Designating the thickness of the drop as h and the frontal area as S, the balance of pressure and surface tension forces requires that:

$$\Delta p S\, \delta h + \sigma \delta S = 0 \tag{3}$$

and rearranging,

$$\frac{\delta S}{\delta h} = -\frac{\Delta p S}{\sigma} \tag{4}$$

The volume of the drop is approximately:

$$V = Sh \tag{5}$$

and differentiating,

$$\frac{\delta S}{\delta h} = -\frac{V}{h^2} = -\frac{S}{h} \tag{6}$$

Combining equations 2, 4 and 6

$$h = \frac{\sigma}{\Delta p} = \frac{2\sigma}{\rho_V (\Delta u)^2} \tag{7}$$

and by equation 5,

$$S = \frac{V}{h} = \frac{\rho_V (\Delta u)^2 V}{2\,\sigma} \tag{8}$$

Substituting equation 8 into equation 1,

$$\Delta u = \left(\frac{4g\,\sigma\Delta\rho}{C_D \rho_V{}^2} \right)^{1/4} \tag{9}$$

Based on an value of CD equal to 1.0, the coefficient $(4g/C_D)^{1/4}$ is equal to the following constants for specific unit systems.

Surface tension in dynes/cm and densities in lb/ft^3 and velocity in ft/sec.

$$(4g/C_D)^{1/4} = 0.73 \tag{10a}$$

Surface tension in dynes/cm and densities in kg/m^3 and velocity in m/sec.

$$(4g/C_D)^{1/4} = 0.445 \tag{10b}$$

Surface tension in Newtons/m and densities in kg/m^3 and velocity in m/sec.

$$(4g/C_D)^{1/4} = 2.50 \tag{10c}$$